

PPPL-2337

PPPL-2337

UC20-G

MICROINSTABILITIES IN WEAK DENSITY GRADIENT TOKAMAK SYSTEMS

By

W.M. Tang, G. Rewoldt, L. Chen

APRIL 1986

PLASMA
PHYSICS
LABORATORY 

PRINCETON UNIVERSITY
PRINCETON, NEW JERSEY

PREPARED FOR THE U.S. DEPARTMENT OF ENERGY,
UNDER CONTRACT DE-AC02-76-CND-3073.

NOTICE

This report was prepared as an account of work sponsored by the United States Government. Neither the United States nor the United States Department of Energy, nor any of their employees, nor any of their contractors, subcontractors, or their employees, makes any warranty, express or implied, or assumes any legal liability or responsibility for the accuracy, completeness or usefulness of any information, apparatus, product or process disclosed, or represents that its use would not infringe privately owned rights.

Printed in the United States of America

Available from:

National Technical Information Service
U.S. Department of Commerce
5285 Port Royal Road
Springfield, Virginia 22161

Price Printed Copy \$ * ; Microfiche \$4.50

<u>*Pages</u>	<u>NTIS Selling Price</u>
1-25	\$7.00
25-50	\$8.50
51-75	\$10.00
76-100	\$11.50
101-125	\$13.00
126-150	\$14.50
151-175	\$16.00
176-200	\$17.50
201-225	\$19.00
226-250	\$20.50
251-275	\$22.00
276-300	\$23.50
301-325	\$25.00
326-350	\$26.50
351-375	\$28.00
376-400	\$29.50
401-425	\$31.00
426-450	\$32.50
451-475	\$34.00
476-500	\$35.50
500-525	\$37.00
526-550	\$38.50
551-575	\$40.00
567-600	\$41.50

For documents over 600 pages, add \$1.50 for each additional 25-page increment.

Microinstabilities in weak density gradient tokamak systems

MASTER

W.M. Tang, G. Rewoldt, and Liu Chen

Plasma Physics Laboratory, Princeton University,

P. O. Box 451, Princeton, New Jersey 08544

PPPL--2337

DE86 011168

ABSTRACT

A prominent characteristic of auxiliary-heated tokamak discharges which exhibit improved ("H-mode type") confinement properties is that their density profiles tend to be much flatter over most of the plasma radius. Despite this favorable trend, it is emphasized here that, even in the limit of zero density gradient, low-frequency microinstabilities can persist due to the nonzero temperature gradient.

I. INTRODUCTION

Experimental results from a number of tokamak devices¹⁻³ have indicated that the so-called "H-mode" beam-heated discharges (which exhibit significantly improved energy confinement properties compared to the more common "L-mode" cases) are characterized by relatively flat density profiles over a large portion of the plasma radius. The present work deals with the question of what types of kinetic instabilities are expected to persist under these conditions. This is an important issue because low-frequency drift-type microinstabilities, which are fundamentally dependent on the strength of the density gradients, have often been proposed as a major contributing cause of the universally observed anomalous electron thermal transport in tokamaks.^{4,5} It should also be kept in mind that, although it is reduced, the observed thermal transport in the H-mode cases remains strongly anomalous.

Since the total pressure gradient is the basic free energy source driving drift-type modes, it is not surprising that instabilities can persist even in the absence of density gradients. In particular, the collisionless trapped-particle mode,⁶ the trapped-electron "ubiquitous" mode,⁷ and the residual trapped-ion mode,⁸ are all examples of pressure-gradient-driven low-frequency microinstabilities in the presence of unfavorable magnetic curvature. In addition to these trapped-particle modes, the well-known ion-temperature-gradient (∇T_i -driven) instabilities⁹ can also be readily excited in a zero-density-gradient region of the plasma. The purpose of this paper is to determine the primary features of the dominant electrostatic instabilities under weak density gradient (and hence large $\eta_j \equiv d \ln T_j / d \ln n_0$) conditions. In Sec. II analytic results are obtained from simplified

model equations in the $\nabla n_0 = 0$ limit to help clarify (i) the relative roles of the interchange and ∇T_i -type destabilizing mechanisms and (ii) the relationship of such instabilities to the conventional trapped-electron drift modes. In Sec. III detailed numerical results from a comprehensive toroidal microinstability code¹⁰ in the electrostatic limit are presented in support of the qualitative trends found in Sec. II. Quasilinear estimates for the anomalous thermal and particle transport diffusivities are also computed here. Finally, possible implications of these results for confinement scaling trends are discussed in Sec. IV.

II. ANALYTIC RESULTS

In order to determine the qualitative (rather than detailed quantitative) properties of the relevant instabilities, a simple local model, which contains the essential physics, is first considered. Following standard procedures,¹¹ the perturbed density responses in the electrostatic limit for the ions and electrons can be approximated by

$$\frac{n_i}{n_0} = \frac{|e|\phi}{T_i} \left[-\frac{\omega_{*i}}{\omega} + \frac{\omega_{di}}{\omega} - \frac{\omega_{*pi}\omega_{di}}{\omega^2} - \left(b_s - \frac{k_{\parallel}^2 c_s^2}{2\omega^2} \right) \left(1 - \frac{\omega_{*pi}}{\omega} \right) \left(\frac{T_i}{T_e} \right) \right], \quad (1)$$

and

$$\frac{n_e}{n_0} = \frac{|e|\phi}{T_e} (1 - i\delta), \quad (2)$$

where ω_{*j} is the diamagnetic drift frequency, $\omega_{*pj} \equiv \omega_{*j} (1 + \eta_j)$, $\omega_{dj} = \omega_{*j} L_n / R =$ magnetic drift frequency, $L_n \equiv -(d \ln n_0 / dr)^{-1}$ is the density gradient scale length, $b_s \equiv k_{\perp}^2 \rho_s^2 / 2$, $\rho_s \equiv c_s / \Omega_i$, $c_s \equiv (2T_e / m_i)^{1/2}$, Ω_i is the ion gyrofrequency, and δ is the dissipative contribution from the nonadiabatic electrons. The usual drift wave ordering is assumed here; i.e., $\omega_{bi}, \omega_{ti} < \omega < \omega_{be}, \omega_{te}$, with ω_{bj} being the average bounce frequency for trapped particles and ω_{tj} being the average transit frequency for circulating particles for each

species. Also, b_s , ω_{dj}/ω , and $k_{\parallel}^2 c_s^2/2\omega^2$ are all taken to be small. In the familiar collision-dominated trapped-electron regime, δ can be approximated by⁶

$$\delta = \epsilon^{3/2} \frac{\omega_{*e} \eta_e}{\nu_{ei}}, \quad (3)$$

with $\epsilon \equiv r/R$ and ν_{ei} being the electron-ion Coulomb collision frequency. In addition, the integral equation nature of the trapped-particle orbit-averaged potential is ignored here; i.e., $\bar{\phi} \rightarrow \phi$. With these simplifying assumptions, the local dispersion relation is easily obtained from the quasineutrality condition and has the form:

$$1 - i\delta - \frac{\omega_{*e}}{\omega} + \frac{\omega_{de}}{\omega} + \frac{\omega_{*pi}\omega_{di}}{\omega^2} \frac{T_e}{T_i} + \left(b_s - \frac{k_{\parallel}^2 c_s^2}{2\omega^2} \right) \left(1 - \frac{\omega_{*pi}}{\omega} \right) = 0. \quad (4)$$

In the conventional limit where $\omega_{*j}/\omega_{dj} \gg 1$ and $\eta_e = O(1)$, the usual result for the dissipative trapped-electron mode⁶ is recovered from Eq.(4); i.e.,

$$\omega \simeq \omega_{*e} + i\epsilon^{3/2} \frac{\omega_{*e}^2 \eta_e}{\nu_{ei}}. \quad (5)$$

However, in the flat density gradient limit, ω_{*j} vanishes, and Eq.(4) reduces to:

$$1 + \frac{\omega_{*i}^T \omega_{di}}{\omega^2} \frac{T_e}{T_i} - \left(b_s - \frac{k_{\parallel}^2 c_s^2}{2\omega^2} \right) \frac{\omega_{*i}^T}{\omega} = 0, \quad (6)$$

with $\omega_{*i}^T \equiv \omega_{*i} \eta_i$. The appropriate ordering in this case is $\omega/\omega_{*i}^T = O(\hat{\epsilon})$ and, as before, δ , ω_{dj}/ω , b_s , and $k_{\parallel}^2 c_s^2/2\omega^2$ are all of order $\hat{\epsilon}$ with $\hat{\epsilon}$ being a smallness parameter. This cubic equation yields unstable modes with the second term and the last term being, respectively, the interchange and ∇T_i destabilizing contributions. Taking $k_{\parallel} \simeq 1/qR$, and defining $L_{Ti} \equiv -(d \ln T_i / dr)^{-1}$ as the ion temperature gradient scale length, it is easy to see that for $(L_{Ti}/R)^{1/2} \gg q^2 b_s$, the familiar η_i -instability⁹ is recovered; i.e., $\omega^3 \simeq -k_{\parallel}^2 c_s^2 \omega_{*i}^T / 2$. For

the opposite limit, $L_{Ti} \ll q^2 b_s$, Eq.(6) yields an electrostatic interchange-type mode with $\omega^2 \simeq -\omega_{*e}^T \omega_{di} T_e / T_i$. Note that for both of these cases, inclusion of the small electron dissipative term, δ , leads to no appreciable modification of the growth rate. This indicates that, in contrast to the usual limit, [Eq.(5)], the influence of collisions on the $\nabla n_0 = 0$ modes is quite weak. Summarily, by examining the simplest local dispersion relation, it is found that, as the density gradient is flattened (and η_i is increased), the dominant electrostatic instability evolves from the conventional dissipative trapped-electron mode to a fluid-like ion mode driven by the interchange and ∇T_i -destabilizing mechanisms. These estimates also indicate that the primary driving process for the flat-gradient modes is ∇T_i at longer wavelengths and interchange (combination of ∇T_i with bad curvature) at shorter wavelengths.

For tokamak systems it is well known that the strongest microinstabilities exhibit a localized or "ballooning" type mode structure along the magnetic field lines.¹¹ In particular, the amplitudes of the relevant eigenfunctions are largest around the magnetic field minimum where the curvature is unfavorable and the bulk of the trapped-particle population is localized. As noted in earlier studies,¹² the ballooning mode formalism¹³ developed to analyze high-mode-number MHD perturbations can be very effectively applied to toroidal microinstability calculations. Using the ballooning representation, the eigenmode equation corresponding to Eq.(6) has the form

$$\left\{ \frac{T_e}{T_i} + \frac{\omega_{*e}^T \omega_{de}}{\omega^2} \left[1 + \left(\hat{s} - \frac{1}{2} \right) \theta^2 \right] + b_s (1 + \hat{s}^2 \theta^2) \frac{\omega_{*e}^T}{\omega} + \frac{1}{2\omega^2} \frac{\omega_{*e}^T}{\omega} \frac{c_s^2}{q^2 R^2} \frac{\partial^2}{\partial \theta^2} \right\} \hat{\phi}(\theta) = 0, \quad (7)$$

with the perturbed potential, $\hat{\phi}(\theta)$, being a nonperiodic function in the domain $-\infty < \theta <$

\propto . The usual analytic model equilibrium¹³ is employed here with $\hat{s} \equiv rq'/q$ being the magnetic shear parameter. In addition, it is assumed that the nonlocal dependence of ω_{di} can be approximated by $\omega_{di} [1 + (\hat{s} - 1/2)\theta^2]$ for strongly ballooning eigenfunctions.

Equation (7) is just the familiar Weber equation yielding the eigenvalue condition

$$1 + \frac{\epsilon_T}{\Omega^2 \tau} + \frac{b_s}{\Omega \tau} = \pm i(2n + 1) \frac{\epsilon_T \hat{s}}{q \Omega^2 \tau} \left[1 + \frac{\epsilon_T}{b_s \Omega} \frac{(\hat{s} - \frac{1}{2})}{\hat{s}^2} \right]^{1/2}, \quad (8)$$

with $\epsilon_T \equiv L_{Ti}/R$, $\Omega \equiv -\omega/\omega_{*i}$, and $\tau \equiv T_e/T_i$. The eigenfunction solution is the Hermite function

$$\hat{\phi}(\theta) \propto H_n(\sigma^{1/2}\theta) \exp(-\sigma\theta^2/2), \quad (9)$$

with $\sigma = \pm ib_s \hat{s} q \Omega / \epsilon_T$. For growing modes [i.e., $\text{Im}(\omega) > 0$], nondivergent solutions require the choice of the lower sign in Eq.(8). Also, recall that in arriving at Eq.(1), the ion sound expansion requires $|k_{\parallel}^2 c_s^2 / 2\omega^2| \ll 1$ or $|(\epsilon_T/q^2 b_s \Omega^2) (1/\hat{\phi}) (\partial^2/\partial\theta^2) \hat{\phi}| \ll 1$. This constraint is best satisfied by considering only the lowest eigenstate, $n = 0$, in Eq.(8).

Provided that $|\hat{s} - 1/2| \ll |b_s \Omega \hat{s}^2 / \epsilon_T|$, Eq.(8) yields the eigenvalue

$$\Omega = i \left(\frac{\epsilon_T}{\tau} \right)^{1/2} \left(1 + i \frac{\hat{s}}{q} \right)^{1/2}. \quad (10)$$

Note that for $|\hat{s}/q| \ll 1$, this reduces to the interchange-dominant result,

$$\Omega \simeq i \left(\frac{\epsilon_T}{\tau} \right)^{1/2}, \quad (11)$$

and for $|\hat{s}/q| \gg 1$, the toroidal η_i -mode is recovered, i.e.,

$$\Omega \simeq \left(\frac{\epsilon_T \hat{s}}{q \tau} \right)^{1/2} \exp(i3\pi/4). \quad (12)$$

III. NUMERICAL RESULTS

In the preceding section, simplified model equations (tractable to analytic solutions) were used to establish the main qualitative features of the instabilities of interest. However, the reliability of such results rests on the degree to which the approximations in the analysis can be justified. To this end, relevant numerical solutions to the actual toroidal integral eigenmode equation have been obtained.

As shown in detail in Ref. 10, general forms of the perturbed distribution function for ions and electrons can be derived from the linearized gyrokinetic equation. These are used in the quasineutrality condition to generate the integral equation governing ballooning-type electrostatic eigenmodes in toroidal systems. Complete trapped-particle dynamics are included in this equation, which is valid for arbitrary mode frequency compared to the particle bounce or transit frequency, and also for arbitrary perpendicular wavelength compared to the particle gyroradius or banana width. Hence, all forms of collisionless dissipation in the form of bounce, transit, and magnetic drift frequency resonances are taken into account here without approximations. With regard to collisional dissipation, an energy and pitch-angle dependent Krook operator which conserves particle number exactly¹⁴ is employed. When applied to the banana regime, this model collision operator¹⁵ can reproduce the results of a Lorentz operator in the limits $|\omega| \ll \nu_{ei}/\epsilon$ and $|\omega| \gg \nu_{ei}/\epsilon$. A detailed description of the non-Hermitian integral equation and the numerical procedure used to solve it is given in Ref. 10 and will not be repeated here. The final eigenmode equation in the electrostatic limit can be written in the form

$$\sum_j Z_j \sum_l M_{l1}^j \hat{\phi}_l = 0, \quad (13)$$

where j labels the particle species and the single-particle charge is $e_j \equiv Z_j e$. Here, $\sum_j Z_j M_{jl}^j$ is the M_{jl}^{11} in Eqs. (44) and (45) of Ref. 10 evaluated using the model MHD equilibrium with circular, concentric magnetic surfaces specified by Eq. (4b) of Ref. 10. The $\hat{\phi}_l$ are the coefficients of the basis functions for the perturbed electrostatic potential eigenfunction, as in Eq. (43) of Ref. 10.

Representative eigenvalues have been numerically computed using input parameters typical of PDX H-mode discharges. Specifically, at a chosen magnetic surface ($r/a = 0.66$) these are: $\epsilon = 0.15$, $T_e = 0.78$ keV, $T_i = 1.05$ keV, $q = 1.27$, $(r/q)(dq/dr) = 0.71$, $k_{\theta}\rho_i = 0.30$, $L_{Te}/r = 0.572$, $L_n/r = 0.572 \times \eta_e$, $\eta_i = 1.11 \times \eta_e$, and $\beta = 0$. Results for normal ($\eta_e = 1$) and flat ($\eta_e = 3.3$ and $\eta_e = 100$) density gradient cases are plotted as a function of the collisionality parameter, $\nu_e^* \equiv \nu_{ei}/\epsilon\omega_{be}$, in Fig. 1. For $\eta_e = 1$, the growth-rate curve exhibits the familiar inverse dependence on collisionality reflected by the estimate given in Eq. (5). However, for the flatter density gradient cases (with corresponding large values of η_i), the instabilities are dominated by fluidlike ion effects, rather than by the electron dissipation. As shown in Fig. 1, the numerical results indeed exhibit the insensitivity to collisional effects predicted by the analytic estimates given in Sec. II [e.g., Eq. (10)]. Comparison of the results for $\eta_e = 3.3$ and $\eta_e = 100$ also supports the fact that once η_i exceeds a critical value (e.g., $\eta_i \gtrsim 2$), the resultant instabilities are quite insensitive to variations in this parameter. The basic trends displayed are found to persist over a wide range of wave numbers, i.e., over a wide range of $k_{\theta}\rho_i$.

In addition to computing the linear properties of the electrostatic instabilities, the corresponding particle and thermal transport has also been estimated. To do this, standard

quasilinear procedures¹⁶ for calculating the relevant fluxes are employed, involving an estimate for the saturated amplitude of the mode, such as that from the familiar ambient gradient or mixing-length approximation, $|\epsilon\phi_0/T_e| \simeq 1/|k_\theta L_{pe}|$, with $L_{pe} \equiv (L_n^{-1} + L_{Te}^{-1})^{-1}$; note that this amplitude is finite even when $\nabla n_0 = 0$. We will leave $|\epsilon\phi_0/T_e|$ unspecified in the results presented here. In particular, the particle and thermal fluxes are obtained in the form:

$$\Gamma_j = \left(\frac{cT_e}{|e|B_0} \right) k_\theta n_0 \left(\frac{\epsilon\phi_0}{T_e} \right)^2 \frac{\text{Im} \sum_{l'} \hat{\phi}_{l'}^* M_{l'l}^j \hat{\phi}_l}{\sum_l |\hat{\phi}_l|^2}, \quad (14)$$

and

$$Q_j = \left(\frac{cT_e}{|e|B_0} \right) k_\theta n_0 \left(\frac{\epsilon\phi_0}{T_e} \right)^2 \frac{\text{Im} \sum_{l'} \hat{\phi}_{l'}^* N_{l'l}^j \hat{\phi}_l}{\sum_l |\hat{\phi}_l|^2}. \quad (15)$$

where $N_{l'l}^j$ is the same as $M_{l'l}^j$ except for an extra factor of E/T_j in the energy integrations (cf. Ref. 10). The corresponding transport coefficients are $D_j \equiv -\Gamma_j/(dn_j/dr)$ and $\kappa_j \equiv -Q_j/[n_j(dT_j/dr)]$. Note that the particle fluxes given by Eq. (14) are automatically ambipolar since $\sum_j e_j \Gamma_j \propto \sum_j Z_j \sum_l M_{l'l}^j \hat{\phi}_l = 0$, from Eq. (13).

Results displaying the transport coefficients corresponding to the eigenvalues of Fig. 1 are shown in Figs. 2, 3, and 4. In Fig. 2, the usual $\eta_e = 1$ case, where trapped-electron modes are dominant, is illustrated. Here, it is seen that κ_e is uniformly larger than κ_i , and that both exhibit the familiar inverse dependence on collisionality for $\nu_e^* \gtrsim 0.2$. In contrast, Fig. 3 shows that, for the flatter density gradient case with $\eta_e = 3.3$, the ion thermal transport tends to be dominant and exhibits very little sensitivity to collisional effects. The numerical results from Fig. 3 are replotted in Fig. 4 with an enlarged vertical scale. The purpose here is to illustrate that, for sufficiently large values of ν_e^* , κ_i remains insensitive to collisionality, but that κ_e , while subdominant, exhibits the expected inverse

collisionality dependence.

IV. CONCLUSIONS

Analytic trends deduced from model equations and supported by detailed numerical results from a comprehensive toroidal microinstability code indicate that as the density gradient is flattened (and η_i is increased), the dominant electrostatic instability evolves from the familiar trapped-electron mode to the ion-temperature-gradient (η_i -type) mode. Specifically, for sufficiently large values of η_i (e.g., $\eta_i \sim 2$), the principal microinstability in toroidal systems is an ion mode driven by the interchange and ∇T_i -destabilizing mechanisms. Unlike the electron drift modes, which are driven by dissipative electron dynamics, these fluidlike instabilities are insensitive to collisions.

The possible implications of the presence of the relevant microinstabilities for energy confinement have been addressed here by estimating the associated thermal diffusivity using the approximations described in Sec. III. As suggested by the results displayed in Figs. 2 to 4, the energy confinement would tend to exhibit a favorable scaling with increasing density for the normal density profile cases where the electron modes are dominant. However, for the flatter gradient cases dominated by toroidal η_i -modes, the sensitivity to collisions (and thus to changes in density) becomes rather weak.

With regard to the specific subject of H-mode confinement, it was confirmed in earlier numerical studies⁵ that the weaker pressure gradients in the interior region of the plasma indeed led to correspondingly weaker instabilities. However, the actual empirical confinement scaling trends of such discharges with parameters such as density have yet to be clearly established. A more striking issue is the question of the nature of the transport

properties in the very steep gradient region at the edge of these plasmas. In order to be consistent with the thermal fluxes computed for the flatter gradient interior zones, the local transport here must be greatly reduced. One possible explanation for such behavior is that finite- β effects associated with the sharp pressure gradient could favorably influence the particle magnetic drifts and thereby reduce the strength of the local mode. A systematic kinetic analysis of such effects for H-mode plasmas is currently in progress.¹⁷

ACKNOWLEDGMENTS

This work was supported by United States Department of Energy Contract No. DE-AC02-76-CHO-3073.

REFERENCES

- ¹ F. Wagner, G. Becker, K. Behringer, D. Campbell, A. Eberhagen, W. Engelhardt, G. Fussmann, O. Gehre, J. Gernhardt, G. v. Gierke, G. Haas, M. Huang, F. Karger, M. Keilhacker, O. Klüber, M. Kornherr, K. Lackner, G. Lisitano, G. G. Lister, H. M. Mayer, D. Meisel, E. R. Müller, H. Murmann, H. Niedermeyer, W. Poschenrieder, H. Rapp, H. Röhr, F. Schneider, G. Siller, E. Speth, A. Stäbler, K. H. Steuer, G. Venus, O. Vollmer, and Z. Yü, *Phys. Rev. Lett.* **49**, 1408 (1982).
- ² M. Nagami, M. Kasai, A. Kitsunozaki, T. Kobayashi, S. Konoshima, T. Matsuda, N. Miya, H. Ninomiya, S. Sengoku, M. Shimada, H. Yokomizo, T. Angel, C. Armentrout, F. Blau, G. Bramson, N. Brooks, R. Chase, A. Colleraine, E. Fairbanks, J. Fasolo, R. Fisher, R. Groebner, T. Hino, R. Hong, G. Jahns, J. Kamperschroer, J. Kim, A. Lieber, J. Lohr, D. McColl, L. Rottler, R. Seraydarian, R. Silagi, J. Smith, R. Snider, T. Taylor, J. Tooker, D. Vaslow, and S. Wojtowicz, *Nucl. Fusion* **24**, 183 (1984).
- ³ S. M. Kaye, *Phys. Fluids* **28**, 2327 (1985).
- ⁴ F. W. Perkins, in *Proceedings of the Fourth International Symposium on Heating in Toroidal Plasmas*, (International School of Plasma Physics and Italian Commission for Nuclear and Alternative Energy Sources, Rome, 1984), p. 977.
- ⁵ W. M. Tang, C. Z. Cheng, J. A. Krommes, W. W. Lee, C. R. Oberman, F. W. Perkins, G. Rewoldt, R. Smith, P. Bonoli, B. Coppi, R. Englade, J. Martinell, and L. Sugiyama, in *Plasma Physics and Controlled Nuclear Fusion Research* (IAEA, Vienna, 1985), Vol. II, p. 213.
- ⁶ B. B. Kadomtsev and O. P. Pogutse, *Nucl. Fusion* **11**, 67 (1971).

- ⁷ B. Coppi and G. Rewoldt, *Phys. Rev. Lett.* **33**, 1329 (1974).
- ⁸ W. M. Tang, J. C. Adam, and D. W. Ross, *Phys. Fluids* **20**, 430 (1977).
- ⁹ L. I. Rudakov and R. Z. Sagdeev, *Dokl. Akad. Nauk SSSR* **138**, 581 (1961) [*Sov. Phys. Dokl.* **6**, 415 (1961)].
- ¹⁰ G. Rewoldt, W. M. Tang, and M. S. Chance, *Phys. Fluids* **25**, 480 (1982).
- ¹¹ W. M. Tang, *Nucl. Fusion* **18**, 1089 (1978).
- ¹² E. A. Frieman, G. Rewoldt, W. M. Tang, and A. H. Glasser, *Phys. Fluids* **23**, 1750 (1980).
- ¹³ J. W. Connor, R. J. Hastie, and J. B. Taylor, *Phys. Rev. Lett.* **40**, 396 (1978).
- ¹⁴ W. M. Tang, G. Rewoldt, and R. J. Hastie, *Bull. Am. Phys. Soc.* **30**, 1559 (1985).
- ¹⁵ J. DeLucia and G. Rewoldt, Princeton Plasma Physics Laboratory Report PPPL-1769 (1981).
- ¹⁶ W. Horton, in *Handbook of Plasma Physics*, edited by M. N. Rosenbluth and R. Z. Sagdeev, Vol.2: Basic Plasma Physics II, edited by A. A. Galeev and R. N. Sudan (Elsevier, New York, 1984), p. 383, cf. Eqs. (10) and (11).
- ¹⁷ G. Rewoldt and W. M. Tang, in *Proceedings of the Sherwood Annual Controlled Fusion Theory Conference*, April 14-16, 1986, New York, NY, abstract 3C25.

FIGURE CAPTIONS

FIG. 1. Typical eigenvalues for drift instabilities dominated by trapped-electron effects ($\eta_e = 1$ curves) and by ion temperature gradient effects ($\eta_e = 3.3$ and $\eta_e = 100$ curves) plotted as a function of the collisionality parameter, $\nu_e^* \equiv \nu_{ei}/\epsilon\omega_{be}$. A complete electrostatic kinetic analysis has been applied here to representative PDX H-mode parameters.

FIG. 2. Transport coefficients corresponding to the $\eta_e = 1$ case plotted against ν_e^* . The right-hand scale for the transport coefficients is $10^6 (\epsilon\phi_0 k_\theta L_{pe}/T_e)^2 \text{ cm}^2 \text{ sec}^{-1}$.

FIG. 3. Transport coefficients corresponding to the $\eta_e = 3.3$ case plotted against ν_e^* . The right-hand scale for the transport coefficients is $10^5 (\epsilon\phi_0 k_\theta L_{pe}/T_e)^2 \text{ cm}^2 \text{ sec}^{-1}$.

FIG. 4. Transport coefficients corresponding to the $\eta_e = 3.3$ case plotted against ν_e^* with an enlarged vertical scale to demonstrate that, for sufficiently large values of ν_e^* , κ_e remains sensitive to collisionality while κ_i is insensitive. The right-hand scale for the transport coefficients is $10^5 (\epsilon\phi_0 k_\theta L_{pe}/T_e)^2 \text{ cm}^2 \text{ sec}^{-1}$.

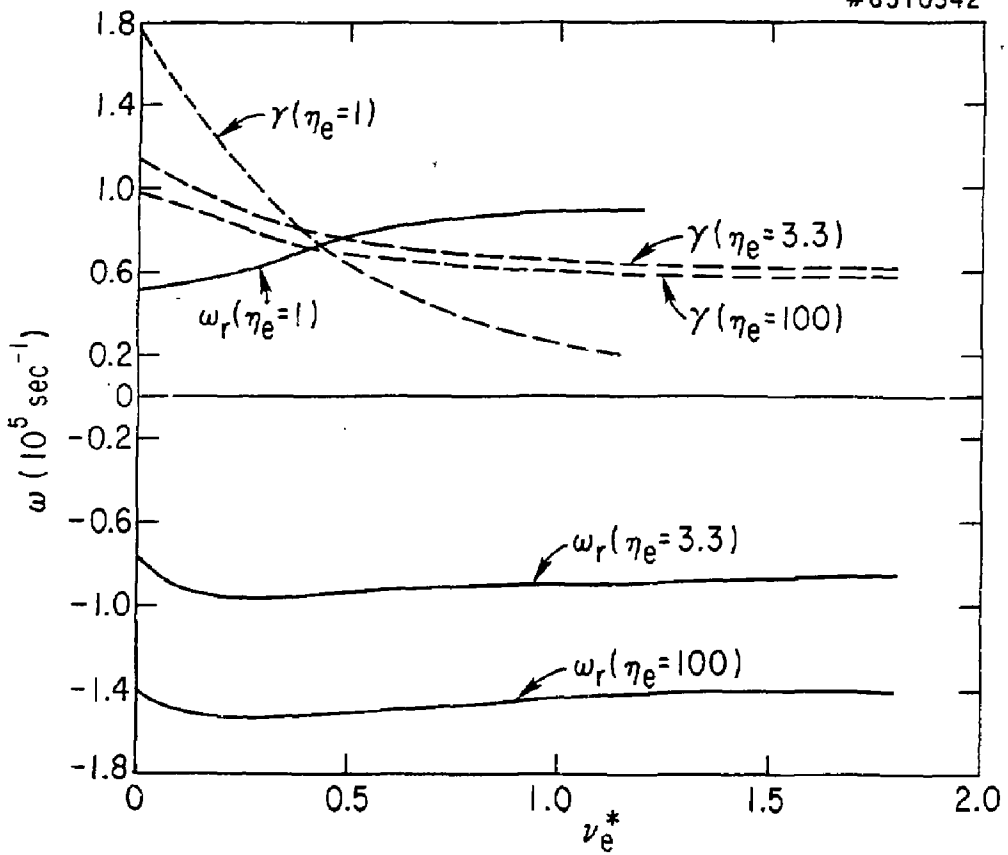


Fig. 1

#86T0066

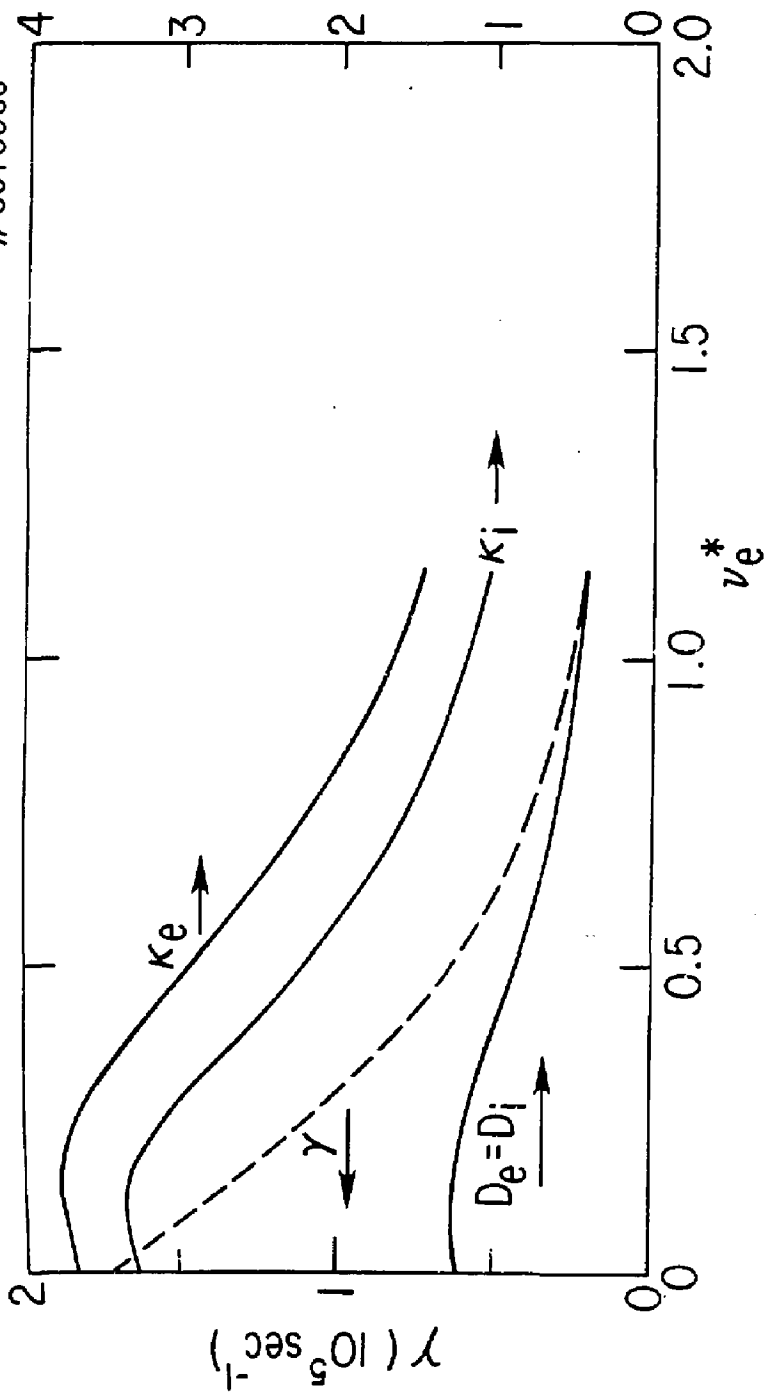


Fig. 2

#86T0065

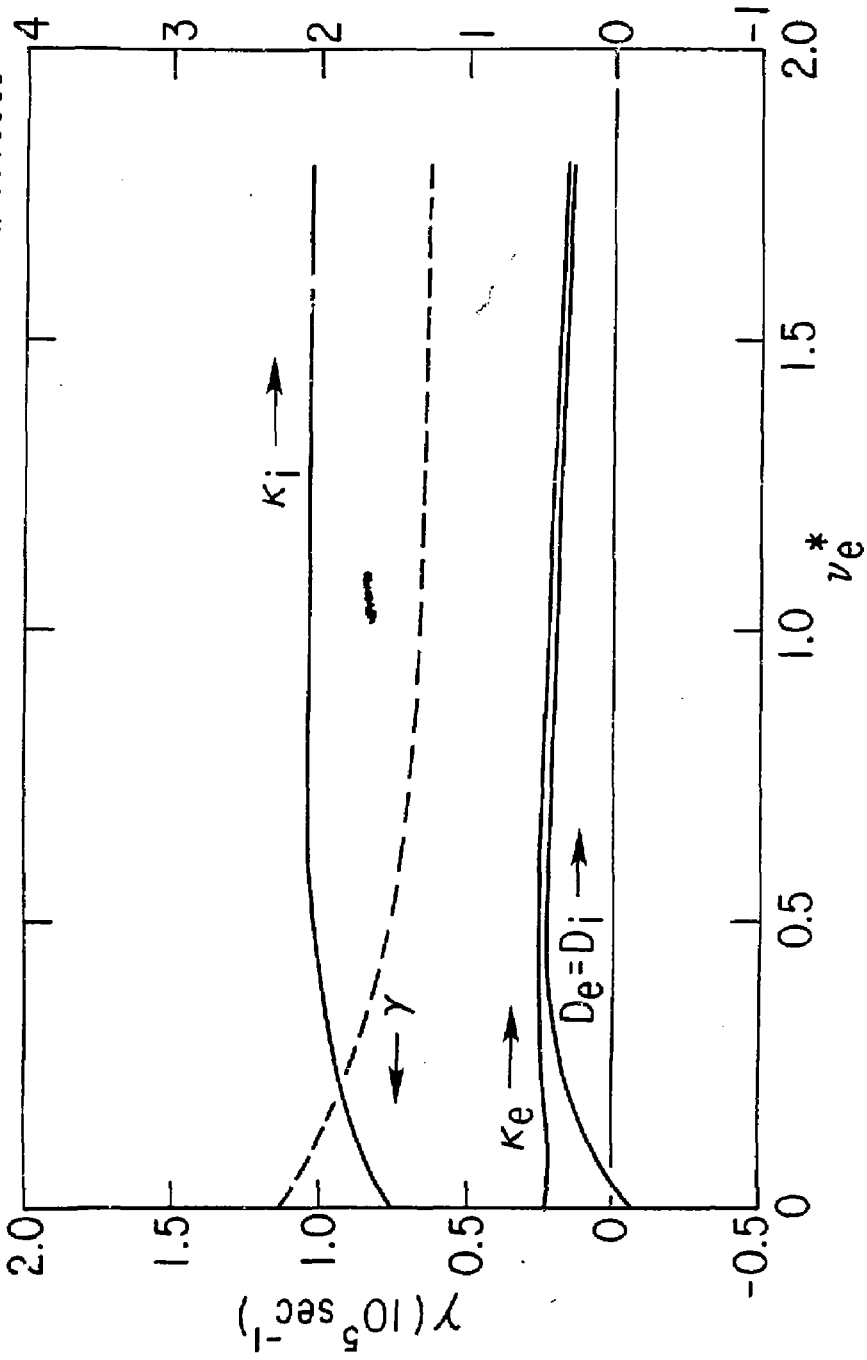


Fig. 3

86T0067

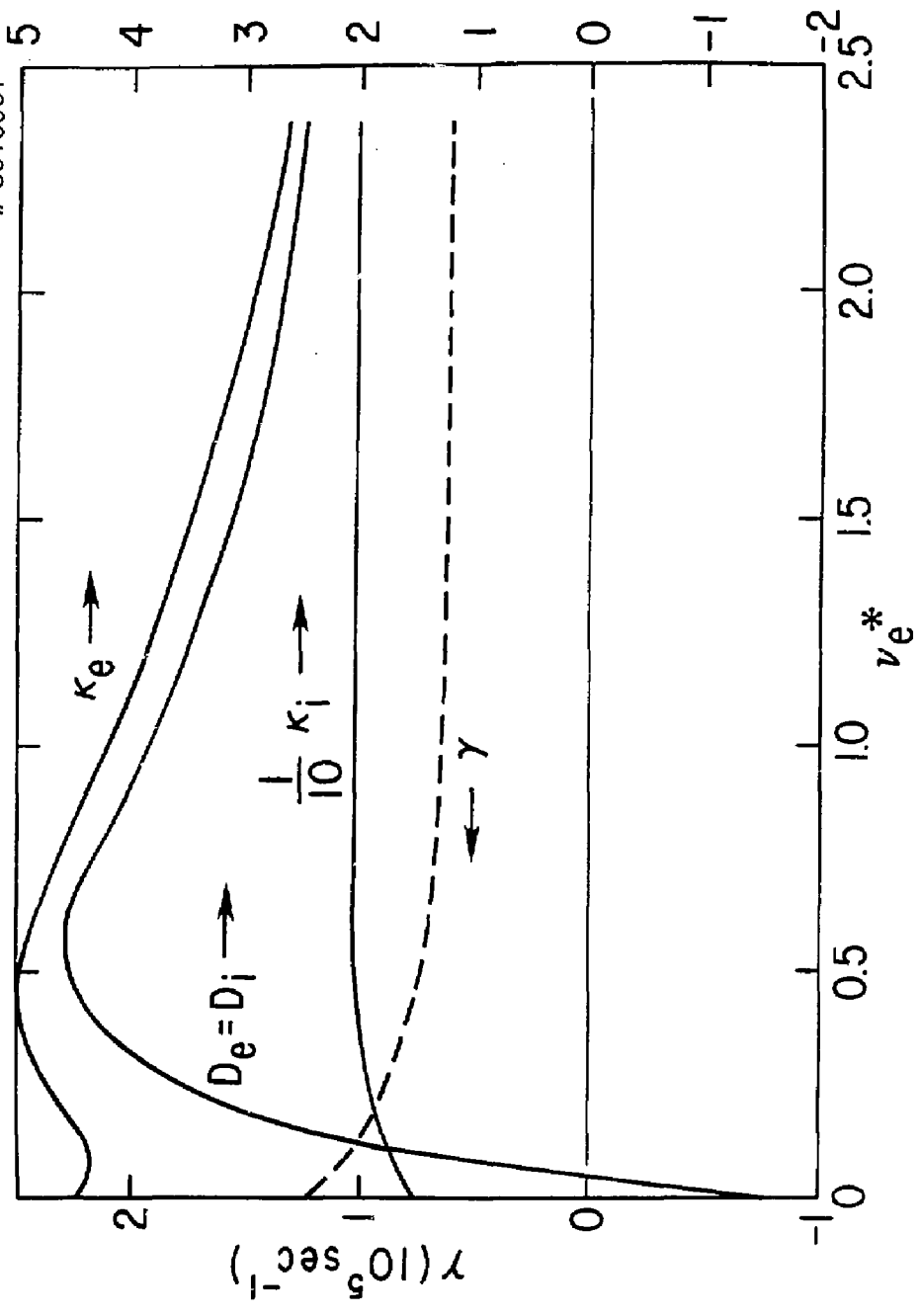


Fig. 4

EXTERNAL DISTRIBUTION IN ADDITION TO UC-20

Plasma Res Lab, Austro Nat'l Univ, AUSTRALIA
Dr. Frank J. Paoloni, Univ of Wollongong, AUSTRALIA
Prof. I.R. Jones, Flinders Univ., AUSTRALIA
Prof. M.H. Brennan, Univ Sydney, AUSTRALIA
Prof. F. Cap, Inst Theo Phys, AUSTRIA
Prof. Frank Verheest, Inst theoretische, BELGIUM
Dr. D. Palumbo, Dj XII Fusion Prog, BELGIUM
Ecole Royale Militaire, Lab de Phys Plasmas, BELGIUM
Dr. P.H. Sakanaka, Univ Estadual, BRAZIL
Dr. C.R. James, Univ of Alberta, CANADA
Prof. J. Teichmann, Univ of Montreal, CANADA
Dr. H.M. Skarsgard, Univ of Saskatchewan, CANADA
Prof. S.R. Sreenivasan, University of Calgary, CANADA
Prof. Tudor W. Johnston, INRS-Energie, CANADA
Dr. Hannes Barnard, Univ British Columbia, CANADA
Dr. M.P. Baciynski, MPB Technologies, Inc., CANADA
Chalk River, Nucl Lab, CANADA
Zhengwu Li, SW Inst Physics, CHINA
Library, Tsing Hua University, CHINA
Librarian, Institute of Physics, CHINA
Inst Plasma Phys, Academia Sinica, CHINA
Dr. Peter Lukac, Komenského Univ, CZECHOSLOVAKIA
The Librarian, Culham Laboratory, ENGLAND
Prof. Schatzman, Observatoire de Nice, FRANCE
J. Radet, CEN-BP6, FRANCE
AM Dupas Library, AM Dupas Library, FRANCE
Dr. Tom Muai, Academy Bibliographic, HONG KONG
Preprint Library, Cent Res Inst Phys, HUNGARY
Dr. R.K. Chhajlani, Vikram Univ. INDIA
Dr. B. Dasgupta, Saha Inst, INDIA
Dr. P. Kaw, Physical Research Lab, INDIA
Dr. Phillip Rosenau, Israel Inst Tech, ISRAEL
Prof. S. Cuperman, Tel Aviv University, ISRAEL
Prof. G. Rostagni, Univ Di Padova, ITALY
Librarian, Int'l Ctr Theo Phys, ITALY
Miss Clelia De Palo, Assoc EURATOM-ENEA, ITALY
Biblioteca, del CNR EURATOM, ITALY
Dr. H. Yamato, Toshiba Res & Dev, JAPAN
Direc. Dept. Lg. Tokamak Dev. JAERI, JAPAN
Prof. Nobuyuki Inoue, University of Tokyo, JAPAN
Research Info Center, Nagoya University, JAPAN
Prof. Kyoji Nishikawa, Univ of Hiroshima, JAPAN
Prof. Sigeru Mori, JAERI, JAPAN
Prof. S. Tanaka, Kyoto University, JAPAN
Library, Kyoto University, JAPAN
Prof. Ichiro Kawakami, Nihon Univ, JAPAN
Prof. Satoshi Itoh, Kyushu University, JAPAN
Dr. D.I. Choi, Adv. Inst Sci & Tech, KOREA
Tech Info Division, KAERI, KOREA
Bibliotheek, Rom-Inst Voor Plasma, NETHERLANDS
Prof. B.S. Lilley, University of Waikato, NEW ZEALAND
Prof. J.A.C. Cabral, Inst Superior Tecn, PORTUGAL
Dr. Octavian Petrus, ALI CUZA University, ROMANIA
Prof. M.A. Hellberg, University of Natal, SO AFRICA
Dr. Johan de Villiers, Plasma Physics, Nucor, SO AFRICA
Fusion Div. Library, JEN, SPAIN
Prof. Hans Wilhelmson, Chalmers Univ Tech, SWEDEN
Dr. Lennart Stanflo, University of UMEA, SWEDEN
Library, Royal Inst Tech, SWEDEN
Centre de Recherches, Ecole Polytech Fed, SWITZERLAND
Dr. V.T. Tolok, Khar'kov Phys Tech Ins, USSR
Dr. D.D. Ryutov, Siberian Acad Sci, USSR
Dr. G.A. Eliseev, Kurchatov Institute, USSR
Dr. V.A. Glukhikh, Inst Electro-Physical, USSR
Institute Gen. Physics, USSR
Prof. T.J.M. Boyd, Univ College N Wales, WALES
Dr. K. Schindler, Ruhr Universitat, W. GERMANY
Nuclear Res Estab, Julich Ltd, W. GERMANY
Librarian, Max-Planck Institut, W. GERMANY
Bibliothek, Inst Plasmaforschung, W. GERMANY
Prof. R.K. Janev, Inst Phys, YUGOSLAVIA